Ordering and phase separation around $Ti_{50}Al_{25}Mo_{25}$ composition in ternary Ti–Al–Mo bcc alloys

P.R. Alonso [a,*], G.H. Rubiolo [a,b]

[a] *Departamento de Materiales, CNEA-CAC, Av. Del Libertador 8250, Buenos Aires (1429), Argentina*
[b] *Dpto. Física, Facultad de Ciencias Exactas y Naturales, Universidad de Buenos Aires, LPMPyMC,
Ciudad Universitaria, Pabellon 1, Buenos Aires (1428), Argentina*

Abstract

The phase equilibria of bcc-based phases in the Ti–Al–Mo alloy system has been studied from first-principles using a combination of ab initio total energy and cluster variation method (CVM) calculations. A set of effective cluster interaction parameters has been derived from the total energies, already computed, of 18 binary and ternary bcc superstructures. These interaction parameters were the input for CVM computation of alloy thermodynamics properties. The CVM has been used to determine the bcc composition–temperature phase diagram in the Ti–Al–Mo system and site preference for bcc-based phases. The investigation focuses its attention on the discussion about the formation of a two-phase field A2 + B2 around the $Ti_{50}Al_{25}Mo_{25}$ composition to suggest some potential directions for future research and development activities on high temperature bcc based superalloys.
© 2003 Elsevier B.V. All rights reserved.

1. Introduction

To improve the performances of aircraft engines and of some nuclear devices, it is necessary to increase service temperature of hot components working in high temperature environments, typically from 827 to 1627 °C (1100 to 1900 K). In this context, research and development activities are underway on a wide range of intermetallic-based alloys systems.

Inspired by the outstanding mechanical performance of superalloys based on elements of the VIIIA group which results from an excellent phase compatibility between their constituent γ and γ' phases, Naka and co-workers [1–3] have attempted to create a γ and γ' type microstructure in a refractory metal-based alloy.

Since refractory metals have a bcc (A2) lattice, a suitable second phase might be of the ordered-cubic-centered B2 type. However, among about 300 binary B2 compounds listed in the literature, no binary B2 compound can be formed with refractory metals. A survey of the literature indicates that the ternary B2 phase has indeed been observed in the Ti–Al–X (X = Cr, Mo, Nb) systems in a wide range of compositions. Their lattice parameters are not well known but seem to be of an order that might lead to a high compatibility with the A2 matrix in the case of Mo and Nb.

In the ternary Ti–Al–Nb, the B2 phase is associated with an order–disorder B2→A2 second-order phase transition. The B2/A2 phase boundary seems to be particularly extended from the Ti-rich to the Nb-rich zones [4,5]. The order–disorder transition temperature is very sensitive to composition; it goes from 600 °C (873 K) for Nb-rich compositions to 1182 °C (1455 K) for Ti-rich compositions [6]. Below 990 °C (1263 K) and for compositions around the stoichiometric Ti_2AlNb a ternary intermetallic compound was identified and designated O phase on the basis of its orthorhombic structure [7]. In view of these properties, it is concluded that the Ti–Al–Nb system cannot provide a γ–γ' type microstructure for a refractory metal-base superalloy.

The B2 phase, in the ternary Ti–Al–Mo, was first reported in the TiAl–MoTi section by Böhm and Löhberg [8] after annealing at 1000 and 800 °C (1273 and 1073 K). The authors associated it with an order–disorder B2→A2 second-order

* Corresponding author.
 E-mail address: pralonso@cnea.gov.ar (P.R. Alonso).

phase transition. Later, Hamajima et al. [9] showed that for a Ti$_{77}$–Al$_{16}$–Mo$_7$ (at%) alloy a structure with B2 particles, having a diameter of approximately 160 Å, surrounded by an A2 matrix was produced upon quenching from 1000 °C (1273 K). When specimens of the alloy were subjected to low-temperature aging (below 773 K), the observed phases were A2, B2 and the disordered-hexagonal α phase. At the aging temperature of about 600 °C (873 K) the B2 phase was no longer present. However, Banerjee et al. [10], working on alloys around the composition Ti$_{48}$–Al$_{47}$–Mo$_5$ (at%) and annealing treatments up to temperatures of 1300 °C (1573 K) followed by quenching in water, did not find the B2 phase although X-ray and electron diffraction characterization were employed. A review of these publications has been presented by Budberg and Schmid-Fetzer [11], who suggested a first-order transformation A2→A2 + B2 leading to the formation of a two-phase field below 1000 °C (1273 K). After the cited review was published, two publications [12,13] have considered the equiatomic Ti–Al region and demonstrated that the substitution of titanium by molybdenum replace single phase γ-TiAl by a two-phase mixture of γ and B2 between 800 and 1400 °C (1073 and 1673 K) (electron diffraction analysis was used to establish the ordered nature of the B2 phase). Instead of this, another publication [14] using X-ray characterization reported a two-phase mixture of γ and A2. It should be noticed that X-ray diffraction experiments could possibly fail to identify B2 peaks due to its low intensity. Given these results and speculations, the ternary Ti–Al–Mo becomes a promising alloy system through the refractory metal-based superalloy approach.

Isothermal cross-sections of the Ti–Al–Mo phase diagram were assessed by calculations in the past. In Refs. [14,15] the authors make use of the regular or subregular models for the solid solutions (CALPHAD method [16]) but they did not consider the experimental information on the ordered phase B2. The phenomenological approach based on a CVM (cluster variation method [17]) treatment of the solid solutions, currently referred as mixed-CVM-CALPHAD method [18], was used in Ref. [19]. Only pair interactions in the limiting binaries fitted from thermodynamics data were considered but a very instructive result is found, a two-phase field A2 + B2 in the inner part of the isotherm at 1000 °C (1273 K).

In this context, we think that a fully first principle phase diagram calculation should be a useful tool.

The modern theory of phase diagram calculations has been possible by great advances in band-structure calculations and theories of configurational thermodynamics and phase transformation. Total energy calculations based on the local density approximation are now sufficiently accurate to explain many properties of materials in terms of the underlying electronic structure [20]. An accurate calculation of the configurational free energy of the alloy is possible within various approximations such as mean-field methods (CVM) or by numerical methods (Monte Carlo simulations [21]).

In these models, it is assumed that the internal energy can be written as a sum of multisite interactions which converge rapidly. Several types of approaches to the calculation of these interactions from first-principles have been developed. One of them chooses a limited set of periodic structures representative for a given problem and their total energies are calculated using self-consistent first-principles calculations. Then, the effective cluster interactions can be obtained from these total energies as suggested by Connolly and Williams [22]. This procedure has been successfully used by Chaumat et al. [23] in the calculation of the bcc Ti–Al–Nb phase diagram.

We have already obtained the ternary cluster expansion of the formation energy in the Ti–Al–Mo system considering all clusters within the tetrahedron approximation of a body-centered-cubic structure [24]. The formation energies of 18 binary and ternary superstructures based on bcc lattices were calculated using the tight-binding-linear-muffin-tin-orbital first-principles-method in the atomic-sphere approximation (TB-LMTO-ASA), including scalar relativistic corrections [25,26]. The set of effective cluster interactions was then derived using the Connolly and Williams approach. As an application of these results, the formation energy of A2 and B2 phases with the same Ti$_{50}$–Al$_{25}$–Mo$_{25}$ composition were evaluated showing, at $T = 0$ K, a higher stability of the B2 compound when compared with the A2 disordered phase.

In this paper we use that result in conjunction with the CVM to determine the bcc composition–temperature phase diagram in the Ti–Al–Mo system. The vibrational effects are not included in these calculations. More particularly, we focus our attention on the discussion about the formation of a two-phase field A2 + B2 around the Ti$_{50}$–Al$_{25}$–Mo$_{25}$ composition.

The remainder of the paper is organized as follows: in Section 2 the basic concepts of the CVM with an irregular tetrahedron as the basic cluster in a bcc structure is presented. In Section 3, the three complete binary phase diagrams involved and three isothermal sections of the ternary phase diagram of the Ti–Al–Mo system are given together with the site occupation in the B2 phase. Section 4 discusses the stability of the two-phase A2 + B2 equilibrium. Finally, the conclusions are presented.

2. Cluster variation method calculations

The CVM is based on the concept of a basic cluster defined as a set of lattice points chosen in such a way that it contains the maximum correlation length to be considered. In the present instance the irregular tetrahedron $\lambda = \{n, m, o, p\}$ is considered to describe the superstructures of the cubic-centered-structures (Fig. 1). Let us define the microcanonical ensemble of the system, $\{\Lambda\}$, built by all arrangements of $N^{\{\lambda\}} = q^{\{\lambda\}}N$ clusters ($q^{\{\lambda\}} = 6$, is the number of clusters $\{\lambda\}$ per lattice point for bcc). A cluster
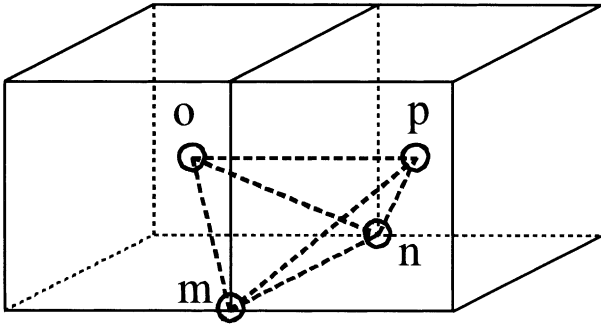
Fig. 1. The irregular tetrahedron cluster in the bcc lattice.

configuration is denoted as $\{i, j, k, l\}$ with species i, j, k, l occupying the positions n, m, o, p, respectively. The following functional for the tetrahedron clusters can be written:

$$F^{\{\Lambda\}} = U^{\{\Lambda\}} - TS^{\{\Lambda\}}$$
$$- \frac{N}{4} \sum_{i,j,k,l} \left(\mu_i^* + \mu_j^* + \mu_k^* + \mu_l^* \right) \rho_{ijkl}^{\{\lambda\}} \qquad (1)$$

where $U^{\{\Lambda\}}$ is the internal energy of the lattice, T the absolute temperature, $S^{\{\Lambda\}}$ is the configurational entropy, μ_i^* is a generalized chemical potential of the species i and $\rho_{ijkl}^{\{\lambda\}}$ represents the probability of the configuration i, j, k, l in the tetrahedron $\{\lambda\}$. The generalized chemical potential is defined as:

$$\mu_i^* = \mu_i - \frac{1}{r} \sum_{i=1}^{r} \mu_i \qquad (2)$$

The key part of the CVM is to calculate the configurational entropy of $\{\Lambda\}$ in terms of the cluster probabilities [17]:

$$S^{\{\Lambda\}} = -q^{\{\lambda\}} N k_B \sum_{i,j,k,l} \rho_{ijkl}^{\{\lambda\}} \ln \rho_{ijkl}^{\{\lambda\}}$$
$$- N k_B \sum_{\nu \subset \lambda} q^\nu a^\nu \sum_{\text{conf}} \rho^\nu \ln \rho^\nu$$

where k_B is the Boltzmann's constant. In this expression the first summation is performed over all configurations of $\{\lambda\}$ and the second summation over all sub-clusters of $\{\lambda\}$ (triplets, pairs and points sub-clusters) and their configurations, the a^ν are the Kikuchi–Barker [27] coefficients for sub-clusters $\{\nu\}$.

The internal energy of the lattice is described, analogously to the entropy, as a functional of the cluster probabilities:

$$U^{\{\Lambda\}} = q^{\{\lambda\}} N \sum_{i,j,k,l} \varepsilon_{ijkl}^{\{\lambda\}} \rho_{ijkl}^{\{\lambda\}}$$

where $\varepsilon_{ijkl}^{\{\lambda\}}$ is the energy of a i, j, k, l configuration in the tetrahedron $\{\lambda\}$.

In order to derive the parameters $\varepsilon_{ijkl}^{\{\lambda\}}$ from thermodynamic data that are usually referred to the mechanical mixture of pure components (like enthalpies of formation

of stoichiometric compounds) the following quantity for a ternary system has to be considered:

$$U^{\{\Lambda\}} - q^{\{\lambda\}} \left(N_A \varepsilon_{AAAA} + N_B \varepsilon_{BBBB} + N_C \varepsilon_{CCCC} \right)$$
$$= q^{\{\lambda\}} N \sum_{i,j,k,l} \omega_{ijkl}^{\{\lambda\}} \rho_{ijkl}^{\{\lambda\}}$$

with

$$\omega_{ijkl}^{\{\lambda\}} = \varepsilon_{ijkl}^{\{\lambda\}} - \frac{1}{4} \sum_{h=i,j,k,l} \varepsilon_{hhhh}^{\{\lambda\}}$$

For each limiting binaries of a ternary system, only four of these parameters are independent corresponding to one possible choice of non-degenerate configuration of ground states AB(B2), AB(B32), A_3B(DO$_3$) and AB$_3$(DO$_3$). The full ternary system description requires six ternary configurations in addition to the 12 binary configurations already mentioned. This six configurations are related to the configurations of ground states L2$_1$ and $F\bar{4}3m$ [28].

It is often preferred to express the tetrahedron energies $\omega_{ijkl}^{\{\lambda\}}$ in terms of pair interactions, adding higher-order cluster interactions as correction terms to the pairs. This leads to the following expansions [29]:

$$\omega_{ijkl}^{\{\lambda\}} = \frac{1}{6} \left(\omega_{ik}^{(1)} + \omega_{il}^{(1)} + \omega_{jk}^{(1)} + \omega_{jl}^{(1)} \right)$$
$$+ \frac{1}{4} \left(\omega_{ij}^{(2)} + \omega_{kl}^{(2)} \right)$$
$$+ \frac{1}{2} \left(\tilde{\omega}_{ijk} + \tilde{\omega}_{ilj} + \tilde{\omega}_{kil} + \tilde{\omega}_{kjl} \right) + \tilde{\omega}_{ijkl}$$

with

$$\omega_{ijkl}^{\{\lambda\}} = \varepsilon_{ij}^{(k)} - \frac{1}{2} \left(\varepsilon_{ii}^{(k)} + \varepsilon_{jj}^{(k)} \right)$$

$$\tilde{\omega}_{ijk} = \tilde{\varepsilon}_{ijk} - \frac{1}{3} \sum_{h=i,j,k} \tilde{\varepsilon}_{hhh}$$

$$\tilde{\omega}_{ijkl} = \tilde{\varepsilon}_{ijkl} - \frac{1}{4} \sum_{h=i,j,k,l} \tilde{\varepsilon}_{hhhh}$$

The (1) and (2) indexes are referred to first and second-order interactions, respectively. The $\tilde{\omega}$ symbols indicate that these are correction terms to the pair interactions. The factors $\frac{1}{6}$, $\frac{1}{4}$, and $\frac{1}{2}$ are due to the fact that each pair or triplet is shared by six, four and two adjoining tetrahedra, respectively. The introduction of pairs and corrections terms formally increases the number of parameters but it must be kept in mind that only 18 energy parameters can be chosen as independent quantities. Any choice of these 18 parameters can be made provided that at least one tetrahedron energy parameter for each ground state is included, otherwise the set becomes dependent.

The set of parameters used in this work links pair interactions to the B2 and DO$_3$ ground states for each limiting binary of the ternary system. For the remaining parameters

Table 1
Interaction parameters of the bcc Ti–Al–Mo system (A = Ti, B = Al, C = Mo; k_BK=8.3145 J/mol)

System	Phase	Strukturbericht designation	Energy of formation [24] (kJ/mol)	Interaction parameters		
				Designation	(k_BK)	(kJ/mol)
Binaries:						
Ti–Al	TiAl	B2	−40.46	$\tilde{\omega}_{ABAB}$	243.53	2.03
	TiAl	B32	−15.95	$\tilde{\omega}_{ABBB}$	336.11	2.80
	Ti$_3$Al	DO$_3$	−24.17	$\omega_{AB}^{(1)}$	−1216.61	−10.12
	Al$_3$Ti	DO$_3$	−7.40	$\omega_{AB}^{(2)}$	−315.59	−2.62
Al–Mo	AlMo	B2	−2.95	$\tilde{\omega}_{BCBC}$	−757.82	−6.30
	AlMo	B32	−29.85	$\tilde{\omega}_{BCCC}$	−202.24	−1.68
	Mo$_3$Al	DO$_3$	−6.85	$\omega_{BC}^{(1)}$	−88.76	−0.74
	Al$_3$Mo	DO$_3$	3.24	$\omega_{BC}^{(2)}$	378.19	3.15
Ti–Mo	TiMo	B2	−12.35	$\tilde{\omega}_{ACAC}$	−2.24	−0.02
	TiMo	B32	−16.11	$\tilde{\omega}_{ACCC}$	−120.98	−1.01
	Ti$_3$Mo	DO$_3$	−11.09	$\omega_{AC}^{(1)}$	−371.22	3.09
	Mo$_3$Ti	DO$_3$	−17.12	$\omega_{AC}^{(2)}$	−393.97	3.28
Ternary:						
Ti–Al–Mo	Ti$_2$AlMo	L2$_1$	−40.79	$\tilde{\omega}_{CCBA}$	31.82	0.27
	Al$_2$TiMo	L2$_1$	−27.97	$\tilde{\omega}_{CBCA}$	−206.06	−1.71
	Mo$_2$TiAl	L2$_1$	−10.00	$\tilde{\omega}_{BBAC}$	−27.09	−0.23
	Ti$_2$AlMo	($F\bar{4}3m$)	−21.41	$\tilde{\omega}_{BABC}$	−294.19	−2.45
	Al$_2$TiMo	($F\bar{4}3m$)	−27.84	$\tilde{\omega}_{AACB}$	−382.92	−3.18
	Mo$_2$TiAl	($F\bar{4}3m$)	−24.44	$\tilde{\omega}_{ACAB}$	27.61	0.23

the tetrahedron correction terms have been selected. The full relationships between the energies of formation of the stoichiometric compounds and these parameters can be found in Ref. [29]. The interaction parameters of the bcc Ti–Al–Mo system have been calculated using the ground state cohesive energies we obtained via the TB-LMTO-ASA method [24]. The values are given in Table 1.

The first step in the search for equilibrium between two phases is to minimize the functional F (Eq. (1)) with respect to the cluster probabilities under the constraints of constant temperature and generalized chemical potentials $\{\mu^*\}$ (Eq. (2)). The minimization process was performed by the algorithm called natural iteration (NI) method derived by Kikuchi [30]. Given an initial condition the NI algorithm always converges to one of the solutions (there are, in general, many local minima of $F^{\{A\}}$ at given values of the state variables, T and $\{\mu^*\}$). If two different initial conditions converge towards different phases with $F^{\{1\}}$ and $F^{\{2\}}$ values, respectively, and $\Delta F^{\{1,2\}} = F^{\{1\}} - F^{\{2\}} = 0$, then equilibrium between the phases {1} and {2} is found. The process was repeated for all possible two-phase equilibrium states in the system. In order to decide whether a two-phase equilibrium is the more stable one for a certain global composition, the Gibbs energy (G) of the possible mixtures were calculated. The minimum among them defined the true phase equilibrium. The value of G for a mixture was calculated as,

$$G(N, T, \chi_i) = N \sum_{i = A,B,C} \mu_i \chi_i, \qquad (3)$$

where the μ_i values are those of the involved phases.

The scheme described above implies a truncation of the interactions. The question remains whether an improvement in the approximation could lead to a more accurate result. The natural way to accomplish it is to include higher-order correlations, this is increasing the size of the clusters with the constraint that superlattice stoichiometries can be described. Being this a bcc system, one appropriate extension is the octahedron truncation. Alternatively, convergence in configurational energy can be evaluated by the method presented in our previous work concerning Ti–Al–Mo system [24]. We showed that the irregular tetrahedron truncation in a Connolly–Wiliams expansion reproduces the total energy at $T = 0$ K of an ordered compound other than the ones contained in the expansion within a minor difference than the convergence limit of the calculation. A proof for the convergence of CVM entropy was presented by Ackerman et al. [31] for multicomponent bcc systems in the tetrahedron approach by finding good agreement with Monte Carlo simulations. This fact allows us to assume that higher order terms in the expansion would be negligible.

3. Results

3.1. Binary diagrams

Fig. 2 shows the metastable calculated bcc phase diagrams Al–Ti, Ti–Mo and Al–Mo superimposed to the experimental equilibrium diagrams [32,33]. The corresponding ground-state ($T = 0$ K) phase diagrams, obtained by means of the tangent method, are also drawn in the same figure.
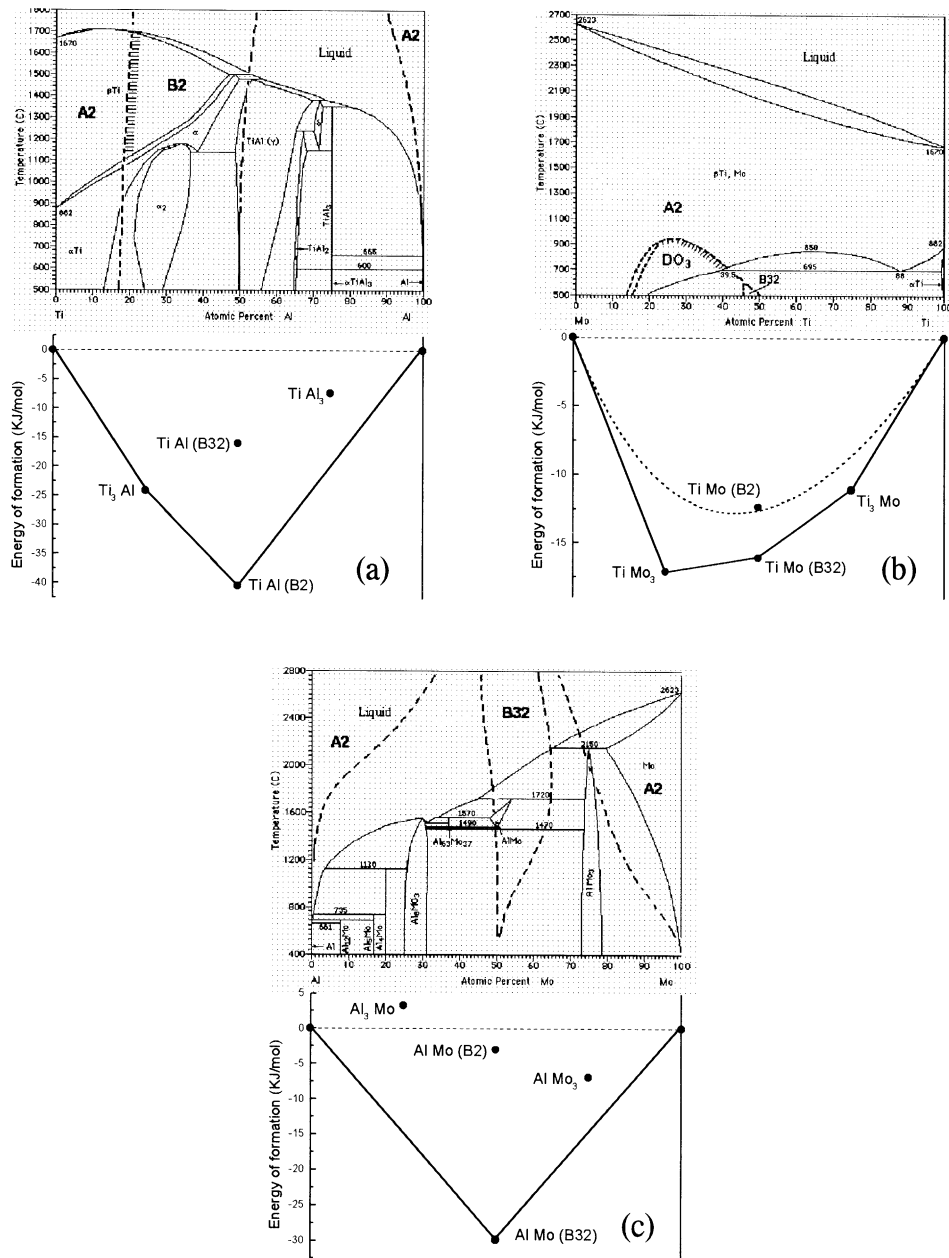
Fig. 2. Binary systems. Ground-state ($T = 0$ K) phase diagram and superposition of the experimental and calculated (bcc) T versus composition phase diagram. (a) Ti–Al, (b) Ti–Mo (the formation energy for A2 phase is shown in dash lines), (c) Al–Mo.

The calculated bcc Ti–Al phase equilibria (Fig. 2a) are metastable, except for a region at high temperatures and aluminum contents ($x_{Al} > 0.19$) where the A2/B2 transition penetrates into the β-Ti phase field. The same theoretical results are reported by Ohnuma et al. [34] and Asta et al. [35]. The existence of the A2/B2 order–disorder transition for $x_{Al} > 0.3$ was confirmed by a combination of calorimetric measurements and theoretical extrapolation of ordering temperature data from Ti–Al–X (X = Cr, Fe) ternary systems [36].

Our results for the Ti–Mo system indicate a negative formation energy for the ordered compounds (Table 1) in agreement with calculations done by Rubin and Finel [37].

The calculated bcc phase diagram (Fig. 2b) predicts ordered phase being stable at low temperature, while a miscibility gap is found experimentally. The existence of the β phase separation has been extensively discussed in the literature, and still remains uncertain [37–39]. Rubin and Finel remark that not only has the miscibility gap been previously much debated but also that there is some ordering evidence from neutron scattering. An inspection of the experimental foundations for β phase separation, together with the analysis of their own experimental results, is done by Furuhara et al. [39]. They conclude that previous data arose from resistivity measurements are not reliable and show that in their

own results there is no evidence for a beta phase separation. They also measured the volume fraction of α phase for a sample with nominal composition of 6.37 at% Mo at 650 °C (923 K), below the proposed monotectoid temperature, finding a value of 42.5%. This leads to the conclusion that beta phase in equilibrium with α phase should have a Mo content of 10.8 at%, instead of the higher Mo content predicted by the phase diagram. Concerning calculated results, a further look into calculated formation energies shows that a miscibility gap cannot be expected from negative values, and also it shows that in cases where the gap is established there is an agreement between experiment and calculation. Au–Ni equilibria, for example, have been calculated with CVM method from ab initio (positive) formation energies by Colinet and Pasturel [40]. In Fig. 2b we show the calculated formation energy (using a Connolly Williams type method as presented in Ref. [24]) for A2 phase at $T = 0$ K together with the corresponding ones for the ordered compounds. It is seen that the energy obtained by the tangent method is below the A2 energy for all compositions. It should also be noted that A2 energy is negative in the whole composition range. The whole analysis leads to the conclusion that there is not enough evidence for the existence of a miscibility gap and that calculated results should be taken into account as an alert for considering equilibria in the Ti–Mo system.

Concerning the Al–Mo system, the calculated bcc equilibria (Fig. 2c) are metastable except within the small existence domain of the compound AlMo which is found experimentally to be A2 instead of B32 as predicted from our calculation.

3.2. Ternary diagrams

In Fig. 3 the ground-state ($T = 0$ K) phase diagram for bcc-based Ti–Al–Mo phases is shown. The ground-state compounds and the three-phase triangles were determined by computing, as function of composition, the combinations of bcc superstructures which minimize the energy. Only the ternary compound Ti_2AlMo with structure $L2_1$ is found to be stable in the ternary ground-state.

Because our previous results on the formation energy in a $Ti_{50}Al_{25}Mo_{25}$ alloy have shown that the ordering sequence would follow the transitions $A2 \rightarrow B2 \rightarrow L2_1$ [24], the isothermal sections to be calculated were chosen after the ordering temperatures for these transitions were known throughout CVM calculations. With this purpose the stability of ordered phases as a function of temperature was calculated starting from the $Ti_{50}Al_{25}Mo_{25}$ composition at low temperature. The order–disorder transition temperatures were found to be 1697 ± 10 °C (1970 ± 10 K) at $Ti_{63}Al_{19}Mo_{17}$ composition and 2627 ± 50 °C (2900 ± 50 K) at $Ti_{64}Al_{16}Mo_{20}$ composition for the $L2_1 \rightarrow B2$ and $B2 \rightarrow A2$ transitions, respectively.

Fig. 4 shows the isothermal sections at 727, 1327 and 1777 °C (1000, 1600 and 2050 K) of the calculated ternary bcc phase diagrams. In the region around $Ti_{50}Al_{25}Mo_{25}$
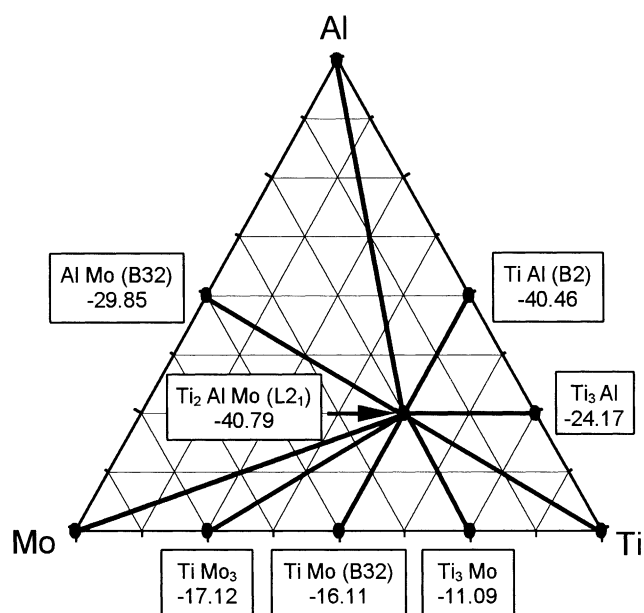

Fig. 3. The Ti–Al–Mo system. Ground-state ($T = 0$ K) phase diagram. The formation energy of each compound is indicated in KJ/mol.

composition, ordering in B2 and $L2_1$ from high temperature A2 is observed. A broad miscibility gap ($L2_1 + A2/B2$) is developed below 1727 °C (2000 K). The $A2 \rightarrow B2$ transformation appears as second-order transition and the B2 phase only forms a two-phase field with the $L2_1$ phase. This behavior is better seen in Fig. 5 where the first- and second-order transition temperatures along the vertical section at $x_{Ti} = 0.63$ are shown.

3.3. Site occupation in the ternary alloy

Concerning the crystallography of the B2 compound, Sikora et al. [41] arrived at the conclusion through EXAFS (extended X-ray absorption fine-structure) studies that Ti atoms fill one sublattice in the bcc cell while Al and Mo atoms occupy randomly the other. Accordingly, we assumed that distribution in our previous ground state relative stability study of structures A2, B2 and $L2_1$ for a $Ti_{50}Al_{25}Mo_{25}$ composition alloy [24].

The evolution of Ti and Al atoms site occupation probabilities as a function of temperature is presented in Fig. 6 starting at low temperature with an $L2_1$ structure for the $Ti_{50}Al_{25}Mo_{25}$ composition. Initially, Ti atoms are preferentially found in n and m sites while Al atoms are on o sites. As temperature increases, some Al atoms move from o sites to p sites reaching similar occupation values in both sites at nearly 1697 °C (1970 K). At the same time, the Ti occupation probabilities of n and m sites remain constant. The increase of the Ti occupation probabilities of o and p sites occurs because the composition was not constraint during these CVM calculations. The site occupation probabilities reached at 1970 K differ from those of the starting $L2_1$ structure and describe a B2-like structure.

Fig. 5. Calculated first- and second-order transition temperatures for bcc-based phases along $Ti_{63}Mo_{37}$–$Ti_{63}Al_{37}$ section of the ternary phase diagram.
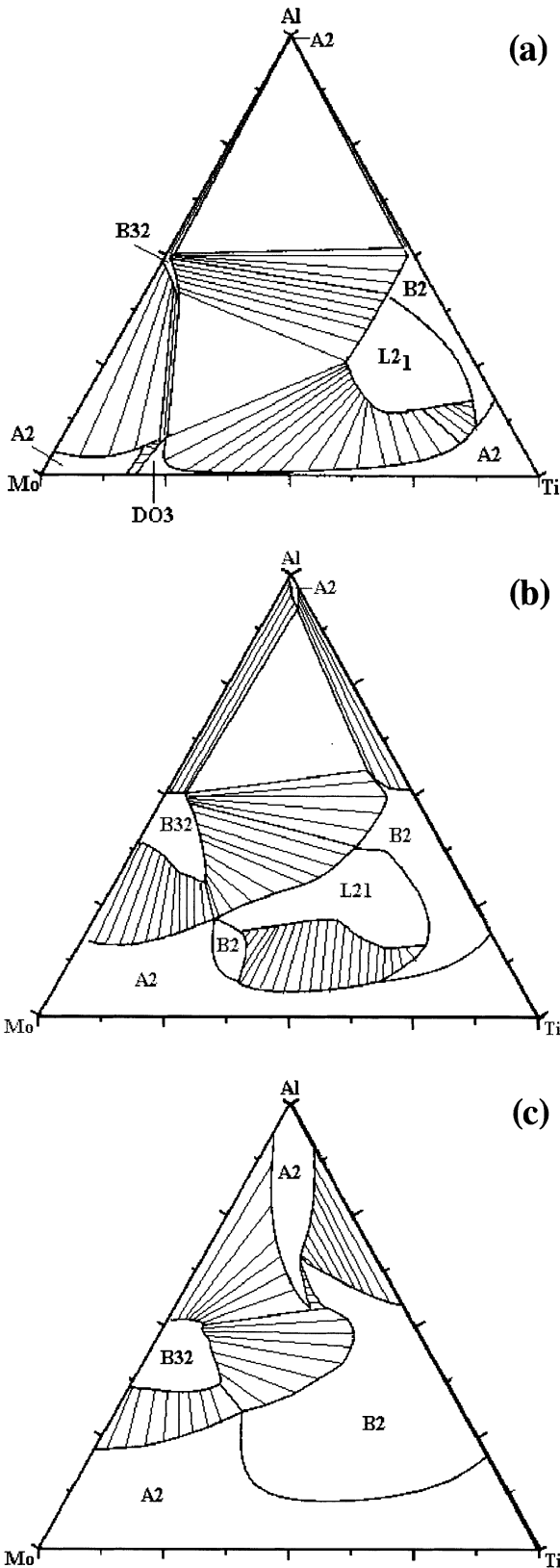

Fig. 4. The Ti–Al–Mo system. Calculated (bcc) T versus composition phase diagram at (a) 727 °C (1000 K), (b) 1327 °C (1600 K) and (c) 1777 °C (2050 K).
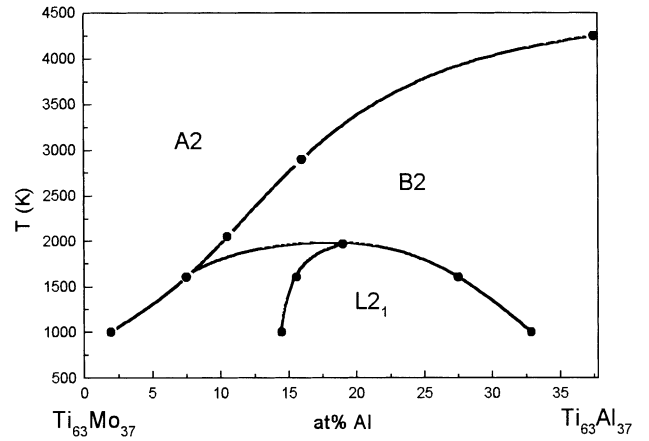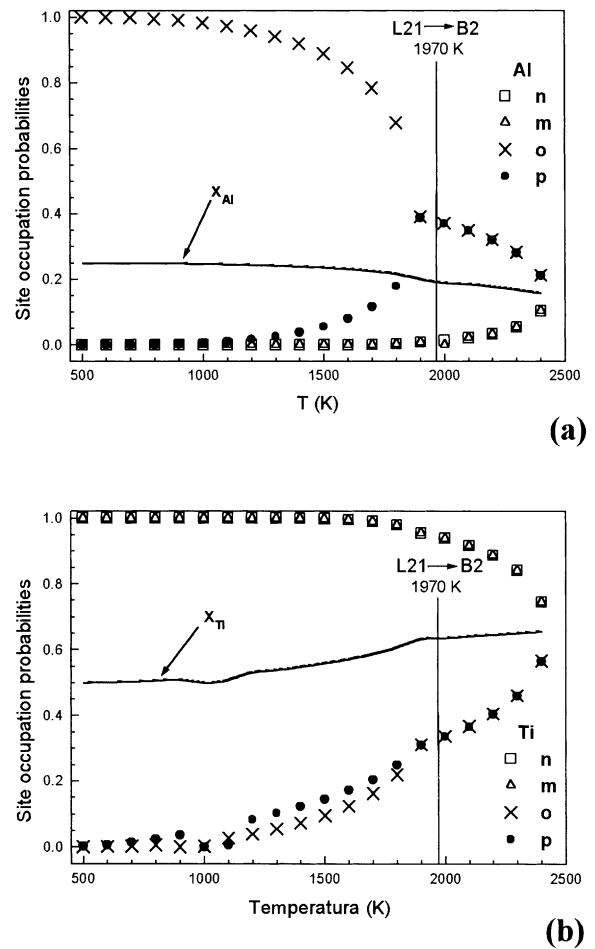

Fig. 6. Site occupation of the $L2_1$ and B2 phase by Al (a) and Ti (b) atoms determined by CVM calculation in the range of compositions and temperatures between $Ti_{50}Al_{25}Mo_{25}$ at 227 °C (500 K) and $Ti_{63}Al_{20}Mo_{17}$ at 1697 °C (1970 K).
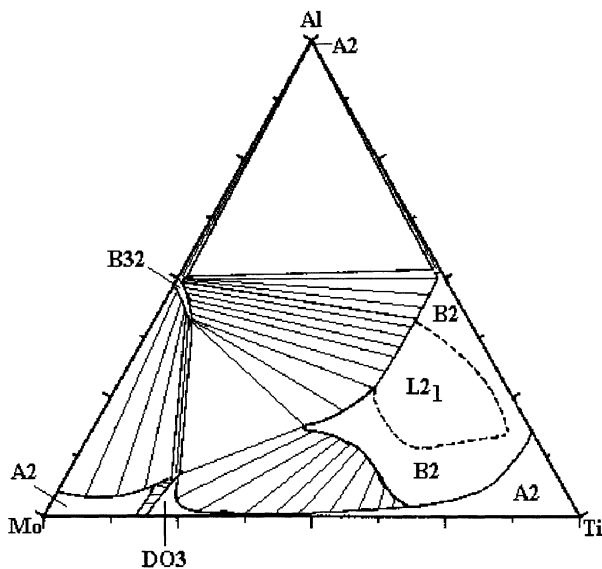
Fig. 7. Calculated metastable equilibrium of the B2 phase in the Ti–Al–Mo system at 727 °C (1000 K).

4. Discussion and conclusions

The values of the interaction parameters in Table 1 have shown that the tetrahedron correction terms are important in front of the pair interactions and cannot be neglected. Unfortunately the first principle values as input of the CVM phase diagram calculations lead to too high B2→A2 order–disorder temperatures with respect to the experimental data. While it is commonplace for mean-field calculations to overestimate transition temperatures by roughly 5–10%, the error in the present case is excessive but follows those obtained by Asta et al. [35] in the Ti–Al–Nb system.

Our calculations predict the formation of a two-phase field A2 + L2$_1$ instead of A2 + B2 as it is suggested in the revised phase equilibrium diagram of Ref. [11]. However, it is worth mentioning that during the evaluation of the metastable equilibrium between A2 and B2 we found a broad miscibility gap (A2 + B2) at 1000 K as shown in Fig. 7. The relative difference between the calculated Gibbs energies (Eq. 3) for the A2 + B2 and A2 + L2$_1$ equilibrium, in the same global composition where both are possible, results of only 2%. This difference is small but enough to discard one equilibrium when compared to the other because the Gibbs energy of each phase in the equilibrium is calculated with an error equal or less than 0.1%. In our opinion, the accuracy in the formation energy's values of the stoichiometric compounds becomes relevant in this case and small changes in its values would do the A2 + B2 equilibrium present instead of the A2 + L2$_1$. This does not mean that the phase L2$_1$ has to disappear but rather an order transition B2→L2$_1$ has to appear. This fact can be observed in the reported literature concerning the Ti–Al–Nb system. While Asta [35] found, for the pseudo-binary TiAl–TiNb section, the phases A2, B2

and L2$_1$ and all phase transitions as second-order, Chaumat et al. [23] found the same phases but with a two-phase field A2 + L2$_1$. The difference between both calculations occurs because the last authors optimized the formation energy's values of the stoichiometric compounds in order to reproduce the B2→A2 order–disorder temperature in agreement with the experimental data; however, the modified values display the same ground state as the one obtained in the ab initio calculations.

Experimentally, the L2$_1$ phase has not been observed in the Ti–Al–Nb system nor in the Ti–Al–Mo system. At low temperature and for composition near Ti$_2$AlNb, the O phase, with an orthorhombic crystal structure [7], is known to be stable and therefore, it was suggested [23] that the formation of L2$_1$ could be suppressed by the formation of this competitive phase. From this knowledge and our results follow that the stability of an O-phase with respect to the phase L2$_1$ (Ti$_2$AlMo) should be investigated experimentally and by means of the electronic structure calculations.

In general, the obtained results are quite encouraging because the formation of a two-phase field between disordered and ordered bcc phases is predicted. Then, the Ti–Al–Mo system becomes a possible candidate for the fabrication of a new superalloy material. Following these theoretical results, we have undertaken an experimental study on two alloys, Ti$_{57}$Al$_{19}$Mo$_{23}$ and Ti$_{62}$Al$_{15}$Mo$_{23}$, which are into the composition zone where a two-phase field could be expected [42]. The work consisted in the fabrication of the alloys by melting the pure components in an arc furnace, thermal treatments and phase's characterization by transmission electron microscopy. The report of this study is underway.

References

[1] S. Naka, M. Thomas, T. Khan, Mater. Sci. Technol. 8 (1992) 291.
[2] S. Naka, T. Khan, Key Eng. Mater. 77–78 (1993) 305.
[3] S. Naka, T. Khan, J. Phase Equilibria 18 (6) (1997) 635.
[4] D.H. Hou, J. Shyue, S.S. Yang, H.L. Fraser, Alloy Modeling and Design, in: G.M. Stocks, P.E.A. Turchi (Eds.), AIME Symposia Proceedings, The Minerals, Metals & Materials Society, Warrendale, 1994, p. 291.
[5] E.S.K. Menon, P.R. Subramanian, D.M. Dimiduk, Metall. Trans. A 27 (1996) 1647.
[6] V. Chaumat, E. Ressouche, B. Ouladdiaf, P. Desre, F. Moret, Scripta Mater. 40 (1999) 905.
[7] D. Banerjee, Prog. Mater. Sci. 42 (1997) 135.
[8] V.H. Böhm, K. Löhberg, Z. Metallkd. 49 (1958) 173.

[9] T. Hamajima, G. Luetjering, S. Weissmann, Metall. Trans. 3 (1972) 2805.

[10] D. Banerjee, R.V. Krishnan, K.I. Vasu, Metall. Trans. 1 (1980) 1095.

[11] P. Budberg, R. Schmid-Fetzer, Ternary Alloys 7 (1993) 229.

[12] S. Das, J.C. Mishurda, W.P. Allen, J.H. Perepezko, L.S. Chumbley, Scripta Met. Mater. 28 (1992) 489.

[13] Z. Chen, I.P. Jones, C.J. Small, Acta Mater. 45 (1997) 3801.

[14] M. Kimura, K. Hashimoto, J. Phase Equlibria 20 (1999) 224.

[15] J.P. Gros, I. Ansara, M. Allibert, E. Alheritiere, Mem. Sci. Rev. Metall 83 (1986) 448.

[16] B. Sundam, B. Jansson, J.O. Anderson, Calphad 9 (1985) 153.

[17] R. Kikuchi, Phys. Rev. 81 (1951) 988.

[18] G. Cacciamani, Y.A. Chang, G. Grimvall, P. Franke, L. Kaufman, P. Miodownik, J.M. Sanchez, M. Schalin, C. Sigli, Calphad 21 (1997) 219.

[19] G. Rubin, A. Finel, J. Phys.: Condens. Matter 5 (1993) 9105.

[20] G.P. Srivastatva, D. Weaire, Adv. Phys. 36 (1987) 463.

[21] K. Binder, Monte Carlo methods in statistical physics, in: K. Binder (Ed.), Springer Series on Topics in Current Physics, Vol. 7, Springer, Berlin, 1986.

[22] J.W.D. Connolly, A.R. Williams, Phys. Rev. B 27 (1983) 5169.

[23] V. Chaumat, C. Colinet, F. Moret, J. Phase Equilibria 20 (1999) 389.

[24] P.R. Alonso, G.H. Rubiolo, Phys. Rev. B 62 (1) (2000) 237.

[25] O.K. Andersen, Phys. Rev. B 12 (1975) 3060.

[26] H.L. Skriver, in: The LMTO Method, Springer–Verlag, Heidelberg, 1984.

[27] J.A. Barker, Proc. R. Soc. London A216 (1953) 45.

[28] G. Inden, W. Pitsch, in: R.W. Cahn, P. Haasen, E.J. Kramer (Eds.), Atomic Ordering in Materials Science and Technology, Vol. 5, VCH Verlagsgesellschaft, Weinheim, 1991, p. 497.

[29] C.G. Schön, Ph.D. thesis, Universität Dortmund, Düsseldorf (1998).

[30] R. Kikuchi, J. Chem. Phys. 60 (1974) 1071.

[31] H. Ackerman, G. Inden, R. Kikuchi, Acta Metall. 37 (1) (1989) 1.

[32] T.B. Massalski, et al., in: 2 Edition, Binary Alloy Phase Diagrams Vol. 3, ASM International, Metals Park, OH, 1991, p. 497.

[33] U.R. Kattner, et al., Metall. Trans. A 23 (8) (1992) 2081.

[34] I. Ohnuma, C.G. Schön, R. Kainuma, G. Inden, K. Ishida, Acta Mater. 46 (6) (1998) 2083.

[35] M. Asta, A. Ormeci, J.M. Wills, R.C. Albers, High Temperature Ordered Intermetallic Alloys-VI, in: MRS Symposia Proceedings, Materials Research Society, Pittsburgh, PA, 1995, p. 157.

[36] I. Ohnuma, Y. Fujita, H. Mitsui, K. Ishikawa, R. Kainuma, K. Ishida, Acta Mater. 48 (2000) 3113.

[37] G. Rubin, A. Finel, J. Phys.: Condens. Matter 7 (1995) 3139.

[38] in: J.L. Murray (Ed.), Phase Diagrams of Binary Titanium Alloys, ASM International, Metals Park, OH, 1987.

[39] T. Furuhara, T. Makino, Y. Idei, H. Ishigaki, A. Takada, T. Maki, Mater. Trans. JIM 39 (1) (1998) 31.

[40] C. Colinet, A. Pasturel, Z. Metallkd. 89 (12) (1998) 863.

[41] T. Sikora, G. Hug, A.M. Flank, J. Phys. IV Coll. 2 Suppl. J. Phys. III 6 (1996) C2–15.

[42] P.R. Alonso, Ph.D. thesis, Instituto de Tecnología 'Jorge A. Sábato', Comisión Nacional de Energía Atómica—Universidad Nacional Gral. San Martín (Argentina) (2001).